



# Fast-forward scaling of atom-molecule conversion in Bose-Einstein condensates

Jing-Jun Zhu <sup>1</sup> and Xi Chen <sup>1,2,\*</sup>

<sup>1</sup>*International Center of Quantum Artificial Intelligence for Science and Technology (QuArtist)  
and Department of Physics, Shanghai University, 200444 Shanghai, China*

<sup>2</sup>*Department of Physical Chemistry, University of the Basque Country UPV/EHU, Apartado 644, 48080 Bilbao, Spain*

Robust stimulated Raman exact passages are requisite for controlling nonlinear quantum systems, with the wide applications ranging from ultracold molecules, non-linear optics to superchemistry. Inspired by shortcuts to adiabaticity, we propose the fast-forward scaling of stimulated Raman adiabatic processes with the nonlinearity involved, describing the transfer from an atomic Bose-Einstein condensate to a molecular one by controllable external fields. The fidelity and robustness of atom-molecule conversion are shown to surpass those of conventional adiabatic passages, assisted by fast-forward driving field. Finally, our results are extended to the fractional stimulated Raman adiabatic processes for the coherent superposition of atomic and molecular states.

## I. INTRODUCTION

Over the past few decades, coherent control has been considered as a strategic cross-sectional field of research for atomic, molecular, optical physics and photochemistry, providing a set of quantum mechanics based methods for the manipulation of populations by laser pulses typically [1–7]. For example, the coherent control of chemical interactions exemplifies its fascinating applications in chemistry, for manipulating and enhancing the product yield [8]. Another intriguing application is so-called superchemistry, in which the coherent Raman transition generates a molecular Bose-Einstein condensate (BEC) from an atomic BEC [9, 10]. With the advancement of modern quantum technologies, quantum control has also emerged as an essential physical basis for state preparation and manipulation in quantum information science and quantum sensing [11, 12].

In this context, there exist several promising techniques for controlling quantum states coherently, such as, adiabatic passages [1, 4, 6], composite pulses [13, 14], optimal control theory [12] and single-shot shaped pulses [15, 16]. Along with these techniques, the concept of “shortcuts to adiabaticity” (STA) provides an alternative control paradigm that improves the speed and robustness of the control process [17, 18]. In the case of controlled population transfer, methods like, the counter-diabatic (CD) driving [19–21] (alternatively quantum transitionless algorithm [22–24]), invariant-based inverse engineering (IE) [25, 26, 36], fast-forward (FF) scaling [27–29] and dressed state method [30] are capable of speeding up the conventional rapid adiabatic passage (RAP) and stimulated Raman adiabatic passage (STIRAP) in two- and three-level quantum system respectively. Despite the experimental demonstrations in various quantum platforms with nitrogen-vacancy (NV) center spins [31–33], cold atoms [34] and superconducting circuits [35], it is still essential to choose or combine these approaches, depending on specific systems and objectives of the study, using appropriate features, overlaps and relations among them [36, 37].

Quite naturally, the STIRAP and its variants [5, 6] have been exploited to study the magneto- and photo-association

of a BEC, by using partially overlapping pulses (pump and Stokes lasers) to produce complete population transfer between two quantum states of an atom or molecule [38–44]. However, the nonlinearity induced from the three-body collision leads to the dynamical instability and inefficiency with the resulting breakdown of adiabaticity [45–47]. In recent years, the technique of STA [48, 49], in addition to optimal control [52, 53] and adiabatic tracking [50, 51], is considered as preferable options to enhance the stability and efficiency of nonlinear STIRAP.

In this article, we explore the FF scaling of atom-molecule conversion in BECs with inherent second-order nonlinearities, by extending the FF to assist the STIRAP [54, 55]. Using the dark state in the nonlinear  $\Lambda$ -type STIRAP as an ansatz, we construct the FF driving field in the form of the couplings between atomic and molecular BECs. We prove that the combination of FF field and nonlinear STIRAP overcomes the instability and inefficiency of photo- and magneto-association of atomic BEC by averting the unwanted diabatic transitions. Furthermore, the FF driving field can be similarly designed in nonlinear fractional STIRAP (f-STIRAP), generating the coherent superposition of atomic and molecular BECs. Conceptually, the FF scaling approach in nonlinear STIRAP is different from the CD driving in linear STIRAP, though they have similar form and presumably similar physical implementation. The instantaneous eigenstates are degenerate and non-orthogonal in the nonlinear systems, resulting in obscure calculation of CD field. In comparison to the original CD field, the derived FF field is also more general and efficient with extra control parameters. Moreover, using the FF scaling approach in nonlinear STIRAP, the state evolution always takes place along the dark state, leaving the excited states unpopulated. This provides the advantage over the IE method [48], where the irreversible losses are inevitable. Finally, we emphasize that our results could be applicable to other nonlinear systems, e.g., nonlinear optics and BEC in an accelerated optical lattice in the presence of the third-order Kerr-type nonlinearities.

In Sec. II, we briefly review the model and Hamiltonian of nonlinear STIRAP and its variants. In Sec. III, we derive the formula of FF driving field accordingly. In Sec. IV, the stability and efficiency of FF assisted STIRAP and f-STIRAP are featured. Finally, we draw the conclusion in Sec. V.

\* xchen@shu.edu.cn

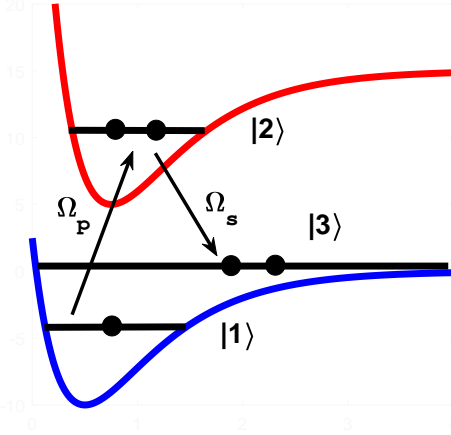


FIG. 1. Schematic representation of coherent two-color photoassociation of a Bose-Einstein condensate in  $\Lambda$ -type STIRAP, where energy level  $|1\rangle$ ,  $|2\rangle$  and  $|3\rangle$  presents the electronic states for the atomic BEC, the excited and stable molecular BECs, respectively,  $\Omega_p$  and  $\Omega_s$  are Rabi frequencies for free-bound and bound-bound transitions.

## II. MODEL, HAMILTONIAN AND ADIABATIC PASSAGE

The Schrödinger equation, describing the nonlinear STIRAP for coherent two-color photoassociation of a BEC in mean-field approximation as shown in Fig. 1, can be expressed as following set of differential equations [48]

$$i\dot{c}_1 = K_1 c_1 + \Omega_p \bar{c}_1 c_2, \quad (1a)$$

$$i\dot{c}_2 = K_2 c_2 + \Delta_p c_2 + \Omega_p c_1^2 + \Omega_s c_3, \quad (1b)$$

$$i\dot{c}_3 = K_3 c_3 + (\Delta_s - \Delta_p) c_3 + \Omega_s c_2, \quad (1c)$$

where  $\Omega_{p,s} \equiv \Omega_{p,s}(t)$  are the time-dependent Rabi frequencies of pump and Stokes fields for free-bound and bound-bound transitions respectively,  $\Delta_{p,s}$  represent the corresponding detunings, and  $c_j$  are the amplitude in state  $|j\rangle$ . Here the overdot represents the derivative with respect to time. Typically, the process of photoassociation aims to remove two atoms from state  $|1\rangle$ , and create a stable molecule in state  $|3\rangle$ , by using the two lasers coupling with a bound-bound molecule in excited state  $|2\rangle$ . The most intriguing property presented here comes from the second-order nonlinearity which appears in the form of pump coupling as well as the third-order Kerr-type nonlinearity,  $K_i = \sum_{j=1}^3 \Lambda_{ij} |c_j|^2$ , with  $\Lambda_{ij}$  being some system dependent constants and populations  $|c_j|^2$ . In the context of atom-molecular conversion in BECs, the extra  $c_1$  and  $\bar{c}_1$  terms appearing in front of  $\Omega_p$  describe the 1 : 2 resonance between the ground atomic state and the excited molecular states. The total population is conserved and is normalized as  $|c_1|^2 + 2(|c_2|^2 + |c_3|^2) = 1$ . Here we write down the Hamiltonian (1) after performing a change of variable  $c_{2,3} \mapsto c_{2,3}/\sqrt{2}$ , yielding the usual normalization,  $|c_1|^2 + |c_2|^2 + |c_3|^2 = 1$  for convenience.

Since the resonance-locking condition,  $\Delta_p = 2K_1 - K_2$  and  $\Delta_s = K_3 - K_2$ , compensates Kerr nonlinear terms with detunings [48], we simplify the previous Hamiltonian, see Eq. (1),

within the on-resonance condition as

$$i\dot{c}_1 = \Omega_p \bar{c}_1 c_2, \quad (2a)$$

$$i\dot{c}_2 = \Omega_p c_1^2 + \Omega_s c_3, \quad (2b)$$

$$i\dot{c}_3 = \Omega_s c_2, \quad (2c)$$

where the second-order nonlinearities are still involved which may lead to the dynamical instability [48, 49]. In principle, there may exist more non-orthogonal eigenstates than the dimension of the Hilbert space in nonlinear systems [46]. Nevertheless, in analogy to its linear counterpart [1, 6], the nonlinear  $\Lambda$ -type STIRAP still supports a dark state (or so-called the coherent population trapping state) with zero eigenvalue [39, 43] which is decoupled from the excited state. Therefore, by setting  $c_2^0 \simeq 0$ , and using  $|c_1^0|^2 + |c_3^0|^2 = 1$ , we obtain the instantaneous population,

$$|c_1^0|^2 = 1 - |c_3^0|^2 = \frac{2\Omega_s}{\Omega_s + \Omega_e}, \quad (3)$$

from which the dark state, corresponding to the eigenvector  $|\Psi_0(t)\rangle = [c_1^0, c_2^0, c_3^0]^T$ , is calculated as  $|\Psi_0(t)\rangle = \mathcal{N}(\Omega_s|1\rangle - c_1^0 \Omega_p |3\rangle)$ , with  $\Omega_e = (\Omega_s^2 + 4\Omega_p^2)^{1/2}$  and  $\mathcal{N}$  being the normalization constant. As used in conventional linear STIRAP [1, 6], the dark state is further reformulated into

$$|\Psi_0(t)\rangle = \cos \Theta(t)|1\rangle - \sin \Theta(t)|3\rangle, \quad (4)$$

with the mixing angle,

$$\Theta(t) = \arctan\left(\frac{c_1^0 \Omega_p}{\Omega_s}\right) = \frac{\sqrt{2}\Omega_p}{\sqrt{\Omega_s(\Omega_s + \Omega_e)}}. \quad (5)$$

This dark state has already been experimentally verified, e.g., through the superposition state of atomic and molecular BECs [44]. Apart from it, we have the other two eigenstates:  $[0, \pm 1/\sqrt{2}, 1/\sqrt{2}]^T$ , with the eigenvalues being  $\pm\Omega_s/2$ . When  $\Omega_s/\Omega_p < 1/\sqrt{2}$ , two more eigenstates exist  $[(1/2 - \Omega_s^2/\Omega_p^2)^{1/2}, \pm 1/\sqrt{2}, \Omega_s/\Omega_p]^T$  which has the eigenvalues  $\pm\Omega_p/\sqrt{2}$ . Due to the lack of orthogonality between the dark state and the other eigenstates, the usual adiabatic condition for linear STIRAP does not hold in the nonlinear case. Thus, one can apply the linear stability analysis only around the fixed stable point [42], which corresponds to the dark state, for calculating three orthogonal eigenstates,  $w_0 = \mathcal{N}_0[-\Omega_s/2, 0, c_1^0 \Omega_p]^T$ , and  $w_{\pm} = \mathcal{N}_{\pm}[c_1^0 \Omega_p, \epsilon_{\pm}, \Omega_s]^T$ . The eigenvalues corresponding to  $w_{0,\pm}$  are  $\epsilon_0 = 0$  and  $\epsilon_{\pm} = \pm\sqrt{\Omega_s \Omega_e}$  respectively.  $\mathcal{N}_{0,\pm}$  are the normalization constants. Accordingly, the adiabatic condition, suitable for the nonlinear STIRAP, is derived as [42],

$$A_{nl} \approx \left(\frac{\mathcal{N}_+}{w_+} + \frac{\mathcal{N}_-}{w_-}\right)^{1/2} \left(\frac{\dot{\Omega}_p \Omega_s - \dot{\Omega}_s \Omega_p}{\Omega_s + \Omega_e}\right) \ll 1. \quad (6)$$

It is straightforward to observe from the adiabatic approximation in Eq. (6), the pump and Stokes Gaussian pulses [1, 6], chosen as

$$\Omega_p(t) = \Omega_0 e^{-(t-\tau)^2/T^2}, \quad (7a)$$

$$\Omega_s(t) = \Omega_0 e^{-(t+\tau)^2/T^2}, \quad (7b)$$

transfer the population from state  $|1\rangle$  at initial time  $t = t_i$  to  $|3\rangle$  at final time  $t = t_f$  along the dark state (4). Note that  $\tau$ ,  $T$ ,  $\Omega_0$  represent the center, width and amplitude of the Gaussian pulses respectively. A more general case would be a combination of one pump and two Stokes Gaussian pulses [56],

$$\Omega_p(t) = \Omega_0 \sin \beta e^{-(t-\tau)^2/T^2}, \quad (8a)$$

$$\Omega_s(t) = \Omega_0 e^{-(t+\tau)^2/T^2} + \Omega_0 \cos \beta e^{-(t-\tau)^2/T^2}, \quad (8b)$$

which asymptotically becomes,

$$0 \xleftarrow{t=-\infty} \frac{\Omega_p(t)}{\Omega_s(t)} \xrightarrow{t=+\infty} \tan \beta. \quad (9)$$

$\Omega_p(t)$  and  $\Omega_s(t)$  creates the coherent superposition of  $|1\rangle$  and  $|3\rangle$  adiabatically by using the dark state. The constant,  $\beta$ , can be determined by the final target state through the combination of Eqs. (5) and (9). Specially for the nonlinear f-STIRAP [57], one has to set  $\beta = \arctan \sqrt{2}$  when the conditions  $\Theta(t_f) = \pi/4$  and  $c_1^0(t_f) = 1/\sqrt{2}$  are stipulated to guarantee the state to be a superposition of  $|1\rangle$  and  $|3\rangle$  with equal amplitude. Generally it takes long time to evolve the system when the adiabatic condition (6) is satisfied, thus spoiling the state by decoherent effect or repeating operation with more energy cost. In what follows, we shall develop the FF scaling approach to speed up the nonlinear STIRAP and f-STIRAP, thus circumventing such difficulties.

### III. FAST-FORWARD SCALING APPROACH

In this section, we shall generalize the FF scaling approach, with the motivation to accelerate the nonlinear STIRAP or f-STIRAP, subjected to a slow variation of pulses. Inspired by the fundamental work of Masuda and Nakamura [27], the FF field for accelerating adiabatic processes have been carried out for several examples like, discrete multi-level quantum system [54, 55] and the nonlinear Gross-Pitaevskii equation or the corresponding Schrödinger equation [58, 59]. In order to recapitulate the FF scaling for our proposal, we choose the dark state (4) as an Ansatz,

$$|\Psi_{FF}(t)\rangle = \cos[\Theta(R(t))]e^{if_1(t)}|1\rangle - \sin[\Theta(R(t))]e^{if_3(t)}|3\rangle, \quad (10)$$

with  $R(t)$  being the ‘‘magnification factor’’ for the rescaled time. The phase factors  $f_{1,3}(t)$  are introduced to satisfy the time-dependent Schrödinger equation,  $i\partial_t|\Psi_{FF}(t)\rangle = H_{FF}(t)|\Psi_{FF}(t)\rangle$ , which comes out to be,

$$i\dot{c}_1 = \Omega_p^{FF} \bar{c}_1 c_2 + \Omega_c^{FF} c_3, \quad (11a)$$

$$i\dot{c}_2 = \Omega_p^{FF} c_1^2 + \Omega_s^{FF} c_3, \quad (11b)$$

$$i\dot{c}_3 = \Omega_c^{*FF} c_1 + \Omega_s^{FF} c_2, \quad (11c)$$

with the modified Rabi frequencies of pump, Stokes and an additional FF fields being  $\Omega_p^{FF} \equiv \Omega_p^{FF}(t)$ ,  $\Omega_s^{FF} \equiv \Omega_s^{FF}(t)$ ,  $\Omega_c^{FF} \equiv \Omega_c^{FF}(t)$  respectively. Here the boundary conditions

$f_{1,3}(t_i) = f_{1,3}(t_f) = 0$  are required to connect to the corresponding adiabatic reference. By inserting this ansatz (10) into the dynamical equation, we have the following equations:

$$\frac{\Omega_p^{FF}(t)}{\Omega_s^{FF}(t)} = \frac{\sin[\Theta(R(t))]}{\cos^2[\Theta(R(t))]} e^{i[\Delta f(t) - f_1(t)]}, \quad (12)$$

$$\frac{d\Delta f(t)}{dt} = \left\{ \frac{2 \cos[2\Theta(R(t))]}{\sin[2\Theta(R(t))]} \right\} \text{Re}[\Omega_c^{FF} e^{i\Delta f(t)}], \quad (13)$$

$$\frac{\partial \Theta}{\partial R} \frac{\partial R}{\partial t} = \text{Im}[\Omega_c^{FF} e^{i\Delta f(t)}]. \quad (14)$$

The Rabi frequencies in the FF scaling approach are finally obtained as

$$\frac{\Omega_p^{FF}(t)}{\Omega_s^{FF}(t)} = \frac{\Omega_p(R(t))}{\Omega_s(R(t))} e^{i[\Delta f(t) - f_1(t)]}, \quad (15)$$

$$\Omega_c^{FF}(t) = e^{-i\Delta f(t)} \left\{ \frac{\sin[2\Theta(R(t))]}{2 \cos[2\Theta(R(t))]} \frac{d\Delta f(t)}{dt} + i \frac{\partial \Theta}{\partial R} \frac{\partial R}{\partial t} \right\}, \quad (16)$$

with  $\Delta f(t) = f_3(t) - f_1(t)$ . When  $f_{1,3}(t) = 0$  is further assumed, the Rabi frequencies can thus be simplified as

$$\frac{\Omega_p^{FF}(t)}{\Omega_s^{FF}(t)} = \frac{\Omega_p(R(t))}{\Omega_s(R(t))}, \quad (17)$$

$$\Omega_c^{FF}(t) = i \frac{\partial \Theta}{\partial R} \frac{\partial R}{\partial t}. \quad (18)$$

Obviously, the additional FF driving field  $\Omega_c^{FF}(t)$  is dependent on the magnification factor and essential for the acceleration of adiabatic passages. The pump and Stokes fields, after FF scaling, constitute the same ratio but with the rescaled time. For  $R(t) = \eta t$ , when the rate of change in  $R(t)$  is small, i.e.,  $\eta \ll 1$ , the adiabatic process is recovered. The FF field vanishes in this limit, i.e.  $\Omega_c^{FF}(t) \simeq 0$ . In the case of  $R(t) = t$ , the FF driving field can be written as  $\Omega_c^{FF}(t) = i\dot{\Theta}$ , which is similar to the CD driving in linear STIRAP [23]. However, the mixing angle is associated with the  $c_1^0$  in Eq. (5) which results in different auxiliary interaction between  $|1\rangle$  and  $|2\rangle$ , distinguishing it from its linear counterpart.

It is important to note that, even though the similarities are predominant between the FF scaling, presented here, and other traditional STA methods like CD driving and IE methods, the differences between them are also significant. Though the additional coupling between  $|1\rangle$  and  $|3\rangle$  are required for both FF scaling and CD driving methods, the FF scaling approach is more general in the sense that when  $f_{13}(t) \neq 0$ , the FF field has both real and imaginary parts with pulse area larger than  $\pi$  [54]. Most importantly, FF scaling approach is fundamentally different from CD driving. In order to obtain the CD term, one has to calculate the non-adiabatic contribution after diagonalizing the Hamiltonian, which is rather straightforward to calculate as the eigen-spectrum is known in linear STIRAP. On the contrary, in nonlinear STIRAP, we can't use the eigenstates and their orthogonality to obtain the CD driving directly. Instead, we assume the dark state as an ansatz for constructing the FF driving field, such that the state transfer is always along the dark state. This also provides significant advantage over the IE method used in Ref. [48], in which the intermediate state  $|2\rangle$  is populated, thus leading

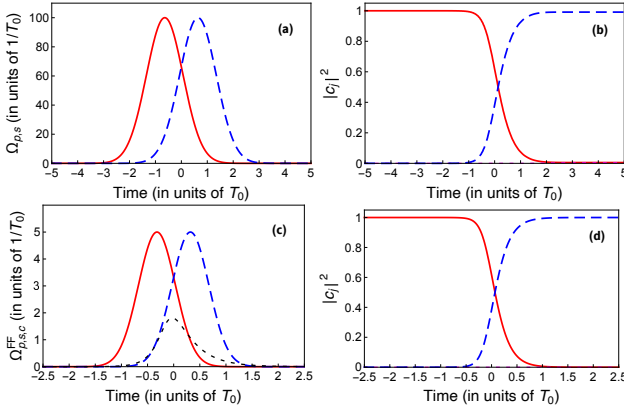


FIG. 2. Nonlinear STIRAP (a) for state transfer (b) from an atomic BEC to a molecular BEC is presented, where  $\Omega_s$  (solid red) and  $\Omega_p$  (dashed blue) sequences are Gaussian type with the amplitude  $\Omega_0 = 100$  (in the units of  $1/T_0$ ),  $\tau = 0.64T$ ,  $T = 1$  (in the units of  $T_0$ ) and  $T_0 = 3.1 \times 10^{-5}$  s. The final population  $|c_3|^2 = 0.9914$  is achieved with total time  $10T$ . For comparison, FF-assisted STIRAP (c) for state transfer (d) is also presented, where  $\Omega_s^{FF}$  (solid red) and  $\Omega_p^{FF}$  (dashed blue) with  $\Omega_0 = 5$  and other parameters are the same. Assisted by the FF driving field  $\Omega_c^{FF}$  (dotted black), the final population  $|c_3|^2 = 0.9999$  is achieved with total time  $5T$ .

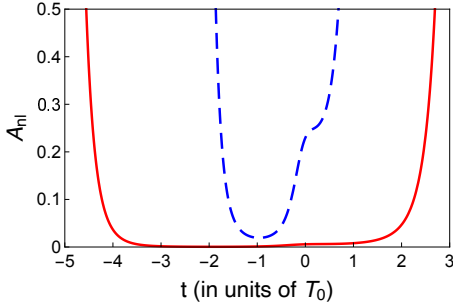


FIG. 3. Parameter  $A_{nl}$  is depicted to quantify the adiabatic condition (6), where the parameters are used for nonlinear STIRAP (solid red) and FF-assisted STIRAP (dashed blue) in Fig. 2.

to the inevitable losses. Moreover, various functions of  $R(t)$  can be further adopted for accelerating the adiabatic passage, which provides more flexibility as well [58, 59]. By selecting the magnification factor  $R(t)$  for the rescaled time, the FF scaling is closely connected with the time-rescaled method, recently proposed in [60]. However, we should point out that the time-rescaled dynamics, driven by the modified fields (17), works perfectly only when the original protocol is adiabatic, since the adiabatic condition cannot be improved without the auxiliary coupling, see Eq. (18).

#### IV. EFFICIENCY AND STABILITY

We first check the conventional nonlinear STIRAP in aforementioned  $\Lambda$ -type nonlinear system. By using Gaussian

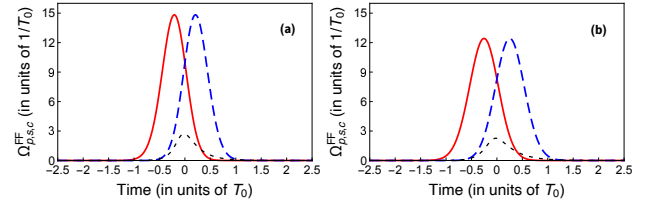


FIG. 4. By using different  $R(t)$ , the modified pump and Stokes Gaussian pulses are presented for nonlinear STIRAP (a,b), together with the assisted FF driving field, where  $\Omega_s^{FF}$  (solid red)  $\Omega_p^{FF}$  (dashed blue) and  $\Omega_c^{FF}$  (dotted black). The parameters are the same as those in Figs. 2. Here (a) and (b) correspond to the trigonometric and polynomial Ansätze of  $R(t)$  respectively.

shapes of pump and Stokes fields, see Eq. (7), the state can be adiabatically transferred from an atomic BEC at initial time  $t_i = -5T$  to a molecular one at  $t_f = 5T$ , as shown in Fig. 2 (a,b), where  $\Omega_0 = 100$  (in the units of  $1/T_0$ ),  $\tau = 0.64T$ ,  $T = 1$  (in the units of  $T_0$ ). Normally,  $T_0 = 3.1 \times 10^{-5}$  s can be chosen in the practical experiment [38], corresponding to  $\Omega_0 = 3.226$  MHz. The final population  $|c_3(t_f)|^2 = 0.9914$  is achieved without exciting the state  $|2\rangle$  when the total time is  $10T$  with the fixed  $\Omega_0 = 100$ . Remarkably, the modified pump/Stokes fields and FF driving field are designed to accelerate the nonlinear STIRAP, as shown in Fig. 2 (c,d), where  $\Omega_0 = 5$ , and other parameters are the same as those in Fig. 2 (a,b). By introducing  $R(t) = at$ , the total evolution time is decreased up to  $5T$  with  $a = 2$ , when assisted by the FF field. From the comparison in Fig. 2, we demonstrate that the assisted FF driving field really speed up the original nonlinear STIRAP, by following the dark state, as seen in population evolution. The final population reaches  $|c_3|^2 = 0.9999$  in Fig. 2 (d), even when the parameters do not fulfill the adiabatic condition (6). In order to quantify the acceleration, we calculate the adiabatic condition (6), see Fig. 3, where  $A_{nl} \ll 1$ , for the parameters that are used in conventional nonlinear STIRAP. When the transfer time is shortened, corresponding parameters make  $A_{nl}$  significantly large so that the adiabaticity is broken, with lower intensities of the pulses. For simplicity, one can choose  $R(t) = t$  while keeping the total time at  $10T$ . It can still be shown that the auxiliary FF field assists the pump and Stokes fields to achieve the high-fidelity state transfer with  $\Omega_0 = 5$ . Here, the Gaussian pulses do not fulfill the adiabatic condition and the FF driving field speeds up the nonlinear STIRAP when  $R(t) = t$ , reducing the system evolution time for small  $\Omega_0$ . This also clarifies the importance of auxiliary coupling, and makes the difference from time-rescaled method [60], as mentioned before.

Moreover, we select other functions of  $R(t)$ , demonstrating the diversity. For instance, one option is trigonometric Ansatz [60],

$$R(t) = at - \frac{t_f - t_i}{2\pi a} (a - 1) \sin \left[ \frac{2\pi a}{t_f - t_i} \left( t - \frac{t_i}{a} \right) \right], \quad (19)$$

where its inverse function and first derivative satisfy the following boundary conditions,  $R^{-1}(t_i) = t_i/a$ ,  $R^{-1}(t_f) = t_f/a$ ,

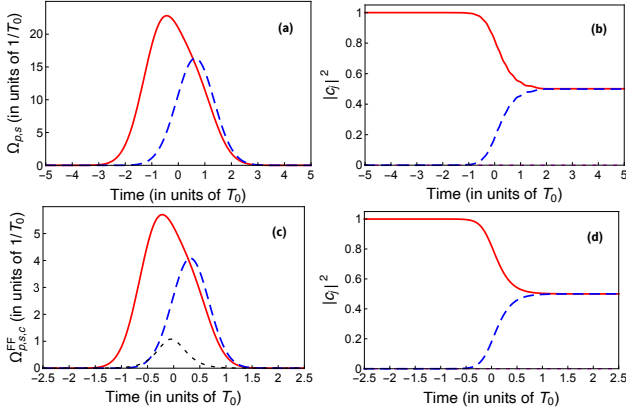


FIG. 5. Nonlinear f-STIRAP (a) for generating the coherent state superposition (b) is presented, where  $\Omega_s$  (solid red) and  $\Omega_p$  (dashed blue) sequences are Gaussian type with the amplitude  $\Omega_0 = 20$  (in the units of  $1/T_0$ ),  $\tau = 0.64T$ ,  $T = 1$  (in the units of  $T_0$ ) and  $T_0 = 3.1 \times 10^{-5}$ s. The superposition of an atomic BEC and a molecular BEC with equal amplitudes is provided with total time  $10T$ . For comparison, FF-assisted f-STIRAP (c) for generating such superposition (d) is also presented, where  $\Omega_s^{FF}$  (solid red) and  $\Omega_p^{FF}$  (dashed blue) with  $\Omega_0 = 5$  and other parameters are the same. Assisted by the FF driving field  $\Omega_c^{FF}$  (dotted black), the superposition of atomic and molecular BECs with equal amplitudes is achieved with total time  $5T$ .

and  $R'(t_i) = R'(t_f) = 1$ . Here the additional conditions on first derivative imply that the time-rescaled Hamiltonian coincides with the original one at initial and final times. Fig. 4 (a) shows the modified pump, Stokes Gaussian pulses for nonlinear STIRAP, and the assisted FF driving field. Here we use  $a = 2$  to compare the results obtained from  $R(t) = 2t$ , by keeping the same fidelity at  $t = t_f$  as that in Fig. 2. We find that the amplitude of Gaussian pulses becomes larger by using the trigonometric function, while the dynamics of population (not shown here) does not change too much. Alternatively, the fourth degree polynomial,  $R(t) = \sum_{i=0}^3 \eta_j t^i$ , can be adopted as well, where the four coefficients  $\eta_j$  are completely solvable by using the aforementioned boundary conditions. We do not write them down explicitly, to avoid the lengthy expression. In this case, the modified pump and Stokes Gaussian pulses are presented in Fig. 4 (b), together with the corresponding FF driving field. It is confirmed by the comparison that the proper choice of  $R(t)$  help decrease the amplitude of pulses.

Next, we also apply the FF driving field for accelerating nonlinear f-STIRAP. In Fig. 5 (a,b) we recover the original adiabatic process to generate the coherent superposition of an atomic BEC and a molecular BEC with equal amplitude where Gaussian pulses of pump and Stokes fields are used, see Eq. (8), with  $\Omega_0 = 20$  and  $\beta = \sqrt{2}$ . Similar to the nonlinear STIRAP, we apply the FF driving field along with the modified pump and Stokes fields to speed up the nonlinear f-STIRAP, see in Fig. 5 (c,d). Here we choose the rescaling function as  $R(t) = 2t$  for simplicity, which can shorten the total evolution time from  $10T$  to  $5T$ , with small coupling amplitude  $\Omega_0 = 5$ . With the assisted FF driving field, the state evolution follows

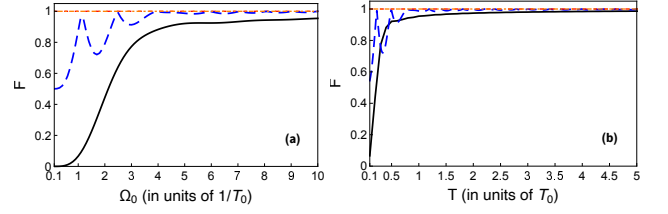


FIG. 6. Fidelity,  $F = |\langle \Psi_0(t_f) | \Psi(t_f) \rangle|^2$ , versus the amplitude  $\Omega_0$  (a) and the width  $T$  (b) of Gaussian pulses, where  $\Psi_0(t_f)$  is target state and  $|\Psi(t_f)\rangle$  is the final solution of time-dependent Schrödinger equation. Here the fidelities of nonlinear STIRAP, nonlinear f-STIRAP and FF-assisted STIRAP are denoted by solid black, dashed blue and dotted red lines, and that of FF-assisted f-STIRAP (dash-dotted orange) are undistinguishable. Other parameters are the same as those in Figs. 2 and 5.

exactly the adiabatic reference in Fig. 5 (b,d) to achieve the perfect coherent superposition with the ratio 1 : 1, but without populating excited state  $|2\rangle$ . It is evident from the Fig. 5 that the FF scaling approach provides desired state superposition, which can be generalized for other ratio of amplitudes as well by changing the parameter  $\beta$  in Eq. (8) through the mixing angle (5).

Finally, we address the issue on efficiency and stability of nonlinear STIRAP and f-STIRAP assisted by the FF driving field. Fig. 6 (a) demonstrates that the fidelity  $F$  depends strongly on the amplitude  $\Omega_0$  of STIRAP and f-STIRAP, where the fidelity can be defined as  $F = |\langle \Psi_0(t_f) | \Psi(t_f) \rangle|^2$ , with  $|\Psi_0(t_f)\rangle$  being the target state (the dark state at  $t = t_f$ ) and  $|\Psi(t_f)\rangle$  being the final solution of time-dependent Schrödinger equation. It is clear that the adiabatic passages do not work for small values of  $\Omega_0$ , due to the breakdown of adiabatic condition. For instance, when  $\Omega_0 = 10$  is chosen, which is much less  $\Omega_0 = 100$ , as used in Fig. 2, the fidelity of nonlinear STIRAP is far away from being unity. Remarkably, the designed FF driving field accelerates the adiabatic passage with perfect fidelity,  $F \simeq 1$ , for arbitrary value of  $\Omega_0$ . In addition, as shown in Fig. 5,  $\Omega_0 = 20$  is required for nonlinear f-STIRAP to meet the adiabatic criteria. With the assisted FF driving, the perfect population transfer can be achieved when  $\Omega_0 = 5$ . However, one has to keep in mind that the energetic cost of STA, that is, the physical constraint on the FF driving field sets the limitation to shorten the time, relevant to quantum speed limits [61]. We also confirm that FF scaling approach improves the stability with respect to the fluctuations in  $T$ , as shown in Fig. 6 (b). The fidelity decreases dramatically for the adiabatic case when  $T$  is shortened, Whereas, ideally, it always remains close to unity, i.e.,  $F \simeq 1$  regardless of the value chosen for  $T$ , when the FF driving field is complemented. Furthermore, the stability with respect to  $\tau$ , affecting the sequence of Gaussian pulses, is improved by the FF driving field as well. For instance, the fidelities are decreased down to  $F = 0.9790$  and  $0.9953$ , respectively, for original nonlinear STIRAP and f-STIRAP, when  $\tau = 0.5T$ . However, with the assisted FF field, the fidelities keep  $F \simeq 1$  in both protocols, where  $T$  is rescaled by magnification factor  $R(t) = 2t$  with the assisted

FF field. Moreover, we check that the other protocols for previously mentioned  $R(t)$  keep the same feature of robustness against variation of  $\Omega_0$  and  $T$ . Actually, the improvement of robustness makes sense as the area of whole pump and Stokes Gaussian pulses is increased by  $\pi$  (for nonlinear STIRAP) and  $\pi/2$  (for nonlinear f-STIRAP) which is induced from the FF driving field. Interestingly, we may simplify the STA recipe in this case, by using a one-photon 1-3 pulse, instead of original two-photon transition [23]. However, the resonant pulses, i.e.  $\pi$  (or  $\pi/2$ ) pulses, are sensitive to parameter fluctuation. As far as physical implementations are concerned, the transition induced from the designed FF driving field can be physically implemented by a magnetic dipole transition, if electric dipole is forbidden. Therefore, the intensity of magnetic field, that directly couples the states  $|1\rangle$  and  $|3\rangle$ , limits the ability to shorten the time infinitely. By combining with the laser fields, the FF driving field, connecting levels  $|1\rangle$  and  $|3\rangle$ , should be on resonance with the Raman transition, which could be problematic due to the phase mismatch and can easily be avoided by shaping the pulses through unitary transformations [34].

## V. CONCLUSION

In summary, we have worked out the FF scaling of coherent control for atom and molecular BECs, with the second-order nonlinearity involved. By using the dark state in nonlinear  $\Lambda$ -type system, we derive the FF driving field which, when combined with the modified pump and Stokes fields, can produce high-fidelity state conversion from an atomic BEC to a molecular one beyond the adiabatic regime. Moreover, the result can be directly generalized to nonlinear f-STIRAP for the coherent superposition of an atomic and a molecular BECs. The FF assisted STIRAP and f-STIRAP have a higher tolerance to the fluctuations in various parameters such as, the intensity and the width of Gaussian pulses. Besides, the original adiabatic passages are speeded up, but without populating the intermediate excited state, which prevents from the losses due to inevitable dissipation [43] or dephasing effect [62].

We must emphasize that the FF scaling approach in nonlinear system are different from CD driving and IE method

of STA. In a nonlinear system, the eigenstates are generally non-orthogonal and degenerate, which hinders the calculation of CD driving, even though the expression of FF field is similar. With extra parameters in the phase of dark state (4), the FF driving provides more flexibility for the atom-molecular conversion, with large area of pulses. We realize that the intermediate state  $|2\rangle$  is populated in an alternative IE method [48], in which one of dynamical modes of Lewis-Riesenfeld invariant for its linear counterpart is applied [63]. However, the price paid in the FF scaling approach is the supplement of the auxiliary coupling between states  $|1\rangle$  and  $|3\rangle$ . And the availability of such coupling will set the limitation to shorten the time. Therefore, when it comes to experimental realization, one can pick up the suitable recipes or protocols as discussed above, taking the physical feasibility and limitations into account. Moreover, there are many choices of magnification factor  $R(t)$  for the rescaled time, which gives different amplitudes of pulses. One can further investigate elsewhere to optimize it with respect to the amplitude of pulses and the robustness against parameter variations, e.g. by using analytical enhanced STA [64] or combining other numerical recipes.

Last but not least, the FF scaling approach is interestingly extended to study fast and robust control of unstable nonlinear systems, such as, BEC in optical lattices with the third-order Kerr-type nonlinearity [65], other applications of coupled waveguides [66, 67] and frequency conversion in nonlinear optics [68] in analogous fashion.

## ACKNOWLEDGMENTS

We thank Koushik Paul for his valuable discussions and comments. We acknowledge the support from NSFC (Grant No. 12075145), STCSM (Grants No. 2019SHZDZX01-ZX04, No. 18010500400, and No. 18ZR1415500), Program for Eastern Scholar, Spanish Government Grant No. PGC2018-095113-B-I00 (MCIU/AEI/FEDER, UE), and Basque Government Grant No. IT986-16. X.C. acknowledges the Ramón y Cajal program (Grant No. RYC2017-22482).

- 
- [1] K. Bergmann, H. Theuer, and B. Shore, *Rev. Mod. Phys.* **70**, 1003 (1998).
  - [2] M. Shapiro and P. Brumer, *Adv. Atom. Mol. Opt. Phys.* **42**, 287-345 (2000).
  - [3] S. Guérin and H. R. Jauslin, *Adv. Chem. Phys.* **125**, 147 (2003).
  - [4] P. Král, I. Thanopoulos, and M. Shapiro, *Rev. Mod. Phys.* **79**, 53 (2007).
  - [5] K. Bergmann, N. V. Vitanov, and B. W. Shore, *J. Chem. Phys.* **142**, 170901 (2015).
  - [6] N. V. Vitanov, A. A. Rangelov, B. W. Shore, and K. Bergmann, *Rev. Mod. Phys.* **89**, 015006 (2017).
  - [7] B. W. Shore, *Manipulating Quantum Structures Using Laser Pulses* Cambridge, Cambridge University Press, 2011.
  - [8] P. Brumer and M. Shapiro, *Ann. Rev. Phys. Chem.* **43**, 257-282 (1992).
  - [9] D. J. Heinzen, R. Wynar, P. D. Drummond, K. V. Kheruntsyan, *Phys. Rev. Lett.* **84**, 5029 (2000).
  - [10] J. J. Hope and M. K. Olsen *Phys. Rev. Lett.* **86**, 3220 (2001).
  - [11] D. D'Alessandro, *Introduction to Quantum Control and Dynamics* (Advances in Applied Mathematics) Chapman and Hall/CRC (2007).
  - [12] S. J. Glaser, U. Boscain, T. Calarco, Christiane P. Koch, W. Kockenberger, R. Kosloff, I. Kuprov, B. Luy, S. Schirmer, T. Schulte-Herbruggen, D. Sugny, and F. K. Wilhelm, *Eur. Phys. J. D* **69**, 279 (2015).
  - [13] M. H. Levitt, *Prog. Nucl. Magn. Reson. Spectrosc.* **18**, 61 (1986).
  - [14] B. T. Torosov, S. Guérin, and N. V. Vitanov, *Phys. Rev. Lett.* **106**, 233001 (2011).
  - [15] E. Barnes and S. Das Sarma, *Phys. Rev. Lett.* **109**, 060401

- (2012).
- [16] D. Daems, A. Ruschhaupt, D. Sugny, and S. Guérin, *Phys. Rev. Lett.* **111**, 050404 (2013).
- [17] D. Guéry-Odelin, A. Ruschhaupt, A. Kiely, E. Torrontegui, S. Martínez-Garaot, and J. G. Muga, *Rev. Mod. Phys.* **91**, 045001 (2019).
- [18] E. Torrontegui, S. Ibáñez, S. Martínez-Garaot, M. Modugno, A. del Campo, D. Guéry-Odelin, A. Ruschhaupt, X. Chen, and J. G. Muga, *Adv. Atom. Mol. Opt. Phys.* **62**, 117 (2013).
- [19] R. Unanyan, L. Yatsenko, K. Bergmann, and B.W. Shore, *Opt. Commun.* **139**, 48-54 (1997).
- [20] M. Demirplak and S. A. Rice, *J. Phys. Chem. A* **107**, 9937 (2003).
- [21] M. Demirplak and S. A. Rice, *J. Chem. Phys.* **129**, 154111 (2008).
- [22] M. V. Berry, *J. Phys. A: Math. Theor.* **42**, 365303 (2009).
- [23] X. Chen, I. Lizuain, A. Ruschhaupt, D. Guéry-Odelin, J. G. Muga, *Phys. Rev. Lett.* **105**, 123003 (2010).
- [24] Y.-C. Li and X. Chen, *Phys. Rev. A* **94**, 063411 (2016).
- [25] A. Ruschhaupt, X. Chen, D. Alonso, and J. G. Muga, *New J. Phys.* **14**, 093040 (2012).
- [26] X.-J. Lu, X. Chen, A. Ruschhaupt, D. Alonso, S. Guérin, and J. G. Muga, *Phys. Rev. A* **88**, 033406 (2013).
- [27] S. Masuda and K. Nakamura, *Proc. R. Soc. A* **466**, 1135 (2010).
- [28] K. Takahashi, *Phys. Rev. A* **89**, 042113 (2014).
- [29] I. Setiawan, B. EkaGunara, S. Masuda, and K. Nakamura, *Phys. Rev. A* **96**, 052106 (2017).
- [30] A. Baksic, H. Ribeiro, and A. A. Clerk, *Phys. Rev. Lett.* **116**, 230503 (2016).
- [31] J. Zhang, J. H. Shim, I. Niemeyer, T. Taniguchi, T. Teraji, H. Abe, S. Onoda, T. Yamamoto, T. Ohshima, J. Isoya, and D. Suter, *Phys. Rev. Lett.* **110**, 240501 (2013).
- [32] B. B. Zhou, A. Baksic, H. Riberio, C. G. Yale, F. J. Heremans, P. C. Jerger, A. Auer, G. Burkard, A. A. Clerk, and D. D. Awschalom, *Nat. Phys.* **13**, 330 (2017).
- [33] J. Kölbl, A. Barfuss, M. S. Kasperczyk, L. Thiel, A. A. Clerk, H. Ribeiro, and P. Maletinsky, *Phys. Rev. Lett.* **122**, 090502 (2019).
- [34] Y. Du, Z. Liang, Y. Chao, X. Yue, Q. Lv, W. Huang, X. Chen, H. Yan, and S.-L. Zhu, *Nat. Commun.* **7**, 12479 (2016).
- [35] A. Vepsäläinen, S. Danilin, G. S. Paraoanu, *Sci. Adv.* **5**, eaau5999 (2019).
- [36] X. Chen, E. Torrontegui, and J. G. Muga, *Phys. Rev. A* **83**, 062116 (2011).
- [37] E. Torrontegui, S. Martínez-Garaot, A. Ruschhaupt, and J. G. Muga, *Phys. Rev. A* **86**, 013601 (2012).
- [38] R. Wynar, R. S. Freeland, D. J. Han, C. Ryu, and D. J. Hainzen, *Science* **287**, 1016 (2000).
- [39] M. Mackie, R. Kowalski, and J. Javanainen, *Phys. Rev. Lett.* **84**, 3803 (2000).
- [40] J. J. Hope, M. K. Olsen, and L. I. Plimak, *Phys. Rev. A* **63**, 043603 (2001).
- [41] P. D. Drummond, K. V. Kheruntsyan, D. J. Heinzen, and R. H. Wynar, *Phys. Rev. A* **65**, 063619 (2002).
- [42] H.-Y. Ling, H. Pu, and B. Seaman, *Phys. Rev. Lett.* **93**, 250403 (2004).
- [43] M. Mackie, K. Härkönen, A. Collin, K.-A. Suominen, and J. Javanainen, *Phys. Rev. A* **70**, 013614 (2004).
- [44] K. Winkler, G. Thalhammer, M. Theis, H. Ritsch, R. Grimm, and J. H. Denschlag, *Phys. Rev. Lett.* **95**, 063202 (2005).
- [45] H. Y. Ling, P. Maenner, W.-P. Zhang, and H. Pu, *Phys. Rev. A* **75**, 033615 (2007).
- [46] J. Liu, B. Wu, and Q. Niu, *Phys. Rev. Lett.* **90**, 170404 (2003).
- [47] A. P. Itin and S. Watanabe, *Phys. Rev. Lett.* **99**, 223903 (2007).
- [48] V. Dorier, M. Gevorgyan, A. Ishkhanyan, C. Leroy, H. R. Jauslin, and S. Guérin, *Phys. Rev. Lett.* **119**, 243902 (2017).
- [49] J.-J. Zhu, X. Chen, H. R. Jauslin, and S. Guérin, *Phys. Rev. A* **102**, 052203 (2020).
- [50] S. Guérin, M. Gevorgyan, C. Leroy, H. R. Jauslin, and A. Ishkhanyan, *Phys. Rev. A* **88**, 063622 (2013).
- [51] M. Gevorgyan, S. Guérin, C. Leroy, A. Ishkhanyan, and H. R. Jauslin, *Eur. Phys. J. D* **70**, 253 (2016).
- [52] M. Vatasescu, O. Dulieu, R. Kosloff and F. Masnou-Seeuws, *Phys. Rev. A* **63**, 033407 (2001).
- [53] X. Chen, Y. Ban, and G. C. Hegerfeldt, *Phys. Rev. A* **94**, 023624 (2016).
- [54] S. Masuda and S. A. Rice, *J. Phys. Chem. A* **119**, 14, 3479-3487 (2015).
- [55] S. Masuda and S. A. Rice, *Adv. Chem. Phys.* **159**, 51-135 (2016).
- [56] N. V. Vitanov, K.-A. Suominen, and B. W. Shore, *J. Phys. B* **32**, 4535 (1999).
- [57] N. Shirkhaghah and M. Saadati-Niari, *Revista Mexicana de Física* **66**, 344 (2020).
- [58] S. Masuda and K. Nakamura, *Phys. Rev. A* **78**, 062108 (2008).
- [59] S. Masuda and K. Nakamura, *Phys. Rev. A* **84**, 043434 (2011).
- [60] Bertúlio de Lima Bernardo, *Phys. Rev. Research* **2**, 013133 (2020).
- [61] O. Abah, R. Puebla, A. Kiely, G. De Chiara, M. Paternostro, and S. Campbell, *New J. Phys.* **21**, 103048 (2019).
- [62] H. Z. Shen, X.-M. Xiu, and X. X. Yi, *Phys. Rev. A* **87**, 063613 (2013).
- [63] A. Benseny, A. Kiely, Y. Zhang, T. Busch, and A. Ruschhaupt, *EPJ Quantum Technology*, **4**, 3 (2017).
- [64] C. Whitty, A. Kiely, and A. Ruschhaupt, *Phys. Rev. Research* **2**, 023360 (2020).
- [65] G.-F. Wang, D.-F. Ye, L.-B. Fu, X.-Z. Chen, and J. Liu, *Phys. Rev. A* **74**, 033414 (2006).
- [66] Y. Lahini, F. Pozzi, M. Sorel, R. Morandotti, D. N. Christodoulides, and Y. Silberberg, *Phys. Rev. Lett.* **101**, 193901 (2008).
- [67] R. Menchon-Enrich, A. Benseny, V. Ahufinger, A. D. Green-tree, T. Busch, and J. Mompart, *Rep. Prog. Phys.* **79**, 074401 (2016).
- [68] H. Suchowski, G. Porat, and A. Arie, *Laser Photon. Rev.* **8**, 333 (2014).